

Symmetric mass generation as a multicritical point with enhanced symmetry

Sandip Maiti  ^{1,2,*} Debasish Banerjee  ^{1,3,†} Shailesh Chandrasekharan  ^{4,‡} and Marina K. Marinkovic  ^{5,§}

¹*Saha Institute of Nuclear Physics, HBNI, 1/AF Bidhannagar, Kolkata 700064, India*

²*Key Laboratory of Quark and Lepton Physics (MOE) and Institute of Particle Physics, Central China Normal University, Wuhan 430079, China*

³*School of Physics and Astronomy, University of Southampton, University Road, SO17 1BJ, UK*

⁴*Department of Physics, Box 90305, Duke University, Durham, North Carolina 27708, USA*

⁵*Institut für Theoretische Physik, Wolfgang-Pauli-Straße 27, ETH Zürich, 8093 Zürich, Switzerland*

(Dated: January 1, 2026)

We explore the phase diagram of a lattice fermion model that exhibits three distinct phases: a massless fermion (MF) phase; a massive fermion phase with spontaneous symmetry breaking (SSB) induced by a fermion bilinear condensate; and a massive fermion phase with symmetric mass generation (SMG). Using the fermion-bag Monte Carlo method on large cubical lattices, we find evidence for traditional second-order critical points separating the first two and the latter two phases. Remarkably, these critical points appear to merge at a multicritical point with enhanced symmetry when the symmetry breaking parameter is tuned to zero, giving rise to the recently discovered direct second-order transition between the massless and symmetric massive fermion phases.

In continuum quantum field theories, relativistic fermions typically acquire masses through explicit fermion bilinear terms in the Lagrangian. When such terms are forbidden by symmetries, fermion masses may still be generated dynamically through the spontaneous breaking of those symmetries [1]. Beginning in the late 1980s, however, it was discovered that massive fermionic phases can emerge in certain lattice models with strictly massless fermions and *without* any spontaneous symmetry breaking, provided the interactions are sufficiently strong [2–4]. These symmetric massive fermion phases were long regarded as lattice artifacts of little relevance to continuum quantum field theory, since the resulting fermion masses typically reside at the lattice cutoff scale.

This perspective has evolved significantly in recent years. Evidence for continuous transitions between the massless fermion phase and the symmetric massive fermion phase has now been found in both purely fermionic theories [5–10] and in models that include gauge interactions [11–13]. At the same time, new insights into anomaly cancellation mechanisms that permit symmetric massive fermion phases have emerged [14–16].

Taken together, these developments suggest the presence of a new fixed point of the RG flow diagram, enabling a nontraditional mass-generation mechanism—now commonly referred to as the SMG—in continuum quantum field theory, whereby fermions acquire masses without spontaneous symmetry breaking [17]. A perturbative study of the RG flows near this new SMG-fixed point using an ϵ -expansion technique has recently been proposed [18]. The SMG mechanism has also renewed interest in compositeness-based approaches to formulating chiral gauge theories on the lattice [19–25].

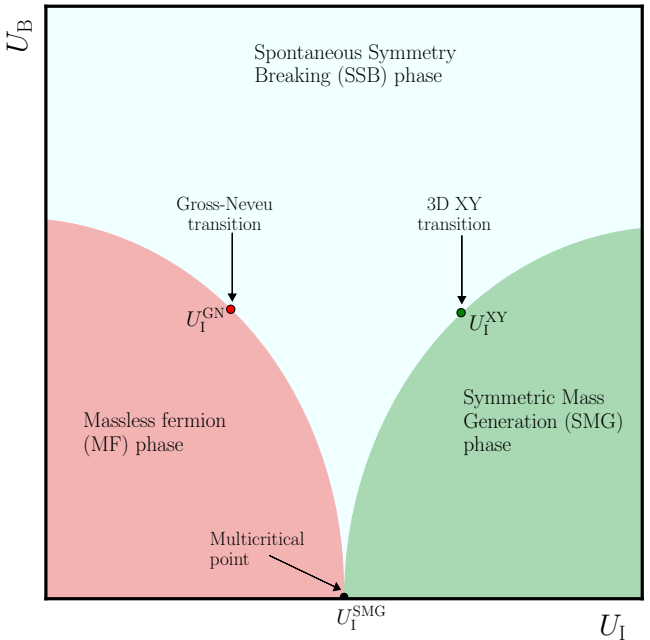


FIG. 1. Phase diagram of the two-flavor massless staggered fermion model in three space-time dimensions with two four-fermion couplings, as defined in Eq. (2). The generic internal symmetry $SU(2) \times SU(2) \times U_\chi(1)$ is enhanced to $SU(4)$ along the $U_B = 0$ axis. The critical point on this axis, which appears as a direct second-order transition between the MF and SMG phases, is in fact a multicritical point where the Gross–Neveu and 3D XY critical lines merge. In the SSB phase the $U_\chi(1)$ symmetry is broken spontaneously.

When a lattice model exhibits both a MF and a SMG phase, the existence of an intermediate phase—where fermions acquire masses through the conventional mechanism of SSB accompanied by a fermion bilinear condensate—cannot be excluded in two or more spatial dimensions. From this perspective, a direct second-order

* sandipmaiti73@gmail.com

† D.Banerjee@soton.ac.uk

‡ sch27@duke.edu

§ marinama@ethz.ch

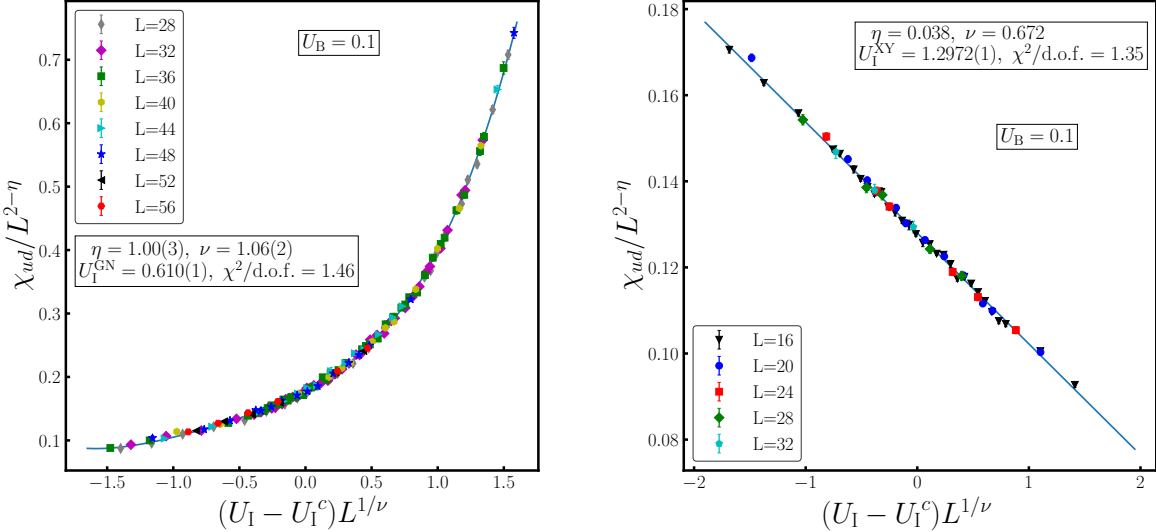


FIG. 2. Plots of the critical finite-size scaling function defined in Eq. (6) at the Gross–Neveu transition (left panel) and the 3D-XY transition (right panel) for $U_B = 0.1$. The solid lines represent polynomial fits: a fourth-order polynomial for the Gross–Neveu case and a linear fit for the 3D-XY case. For the Gross–Neveu transition, the critical coupling and critical exponents are treated as fit parameters, whereas for the 3D-XY transition the critical exponents are fixed to their known values. The Monte Carlo data, shown with error bars, were obtained for various lattice sizes L and a range of couplings U_I in the vicinity of the respective critical points.

transition between the MF and SMG phases would ordinarily require fine tuning of at least two independent parameters, as originally argued in Ref. [26]. It is therefore surprising that in a simple Euclidean lattice model with two flavors of massless staggered fermions, tuning a single local four-fermion coupling U_I appeared to produce such a direct transition [6, 7]. The action of this model is

$$S_1 = \sum_{\langle ij \rangle} \eta_{ij} (\bar{u}_i u_j - \bar{u}_j u_i + \bar{d}_i d_j - \bar{d}_j d_i) - U_I \sum_i (\bar{u}_i u_i \bar{d}_i d_i), \quad (1)$$

where i and j label sites of a three-dimensional cubic lattice, and $\langle ij \rangle$ denotes nearest-neighbor pairs. The staggered fermion fields $\bar{u}_i, u_i, \bar{d}_i$, and d_i are Grassmann-valued, and the phase factors η_{ij} implement a π -flux through each plaquette of the cubic lattice. These fermions are known to describe four massless flavors of four-component Dirac fermions [27].

In order to shed further light on this surprising second-order critical point, in this work we extend Eq. (1) by introducing an additional interaction U_B , modifying the action to

$$S_2 = S_1 - U_B \sum_{\langle ij \rangle} (\bar{u}_i u_i \bar{u}_j u_j + \bar{d}_i d_i \bar{d}_j d_j). \quad (2)$$

The additional coupling U_B allows us to explore the fate of the direct second-order transition between the MF and SMG phases.

Using an extension of the fermion bag algorithm [29], we determine the phase diagram of Eq. (2) in the U_I – U_B plane and find that it contains all three expected phases: the MF phase at small U_I and U_B , the SMG phase at large U_I and small U_B , and an intermediate SSB phase separating them, as shown in Fig. 1. This phase structure clearly demonstrates that the direct second-order transition at $U_B = 0$ reported in earlier studies is in fact a fine-tuned point: a multicritical point where the critical line separating the MF and SSB phases meets the critical line separating the SSB and SMG phases. The transition along the former line is consistent with the three-dimensional Gross–Neveu $U(1)$ universality class involving $N_f = 4$ flavors of four-component Dirac fermions, while the latter line is described by the three-dimensional bosonic XY universality class.

Our calculations are performed on some of the largest lattices studied to date. The Gross–Neveu transition is investigated on cubical lattices with linear size up to $L = 56$, while for the bosonic XY transition—which is known to be particularly challenging to access in a microscopic fermionic model—we are able to simulate lattices up to $L = 32$. Details of the fermion bag Monte Carlo algorithm, together with the data and scaling analysis, are provided in a companion article [28].

The appearance of a finely tuned multicritical point precisely at $U_B = 0$ is again somewhat surprising. Interestingly, however, the lattice model defined in Eq. (2) possesses an enhanced internal symmetry when $U_B = 0$. To understand this enhancement, it is helpful to assign

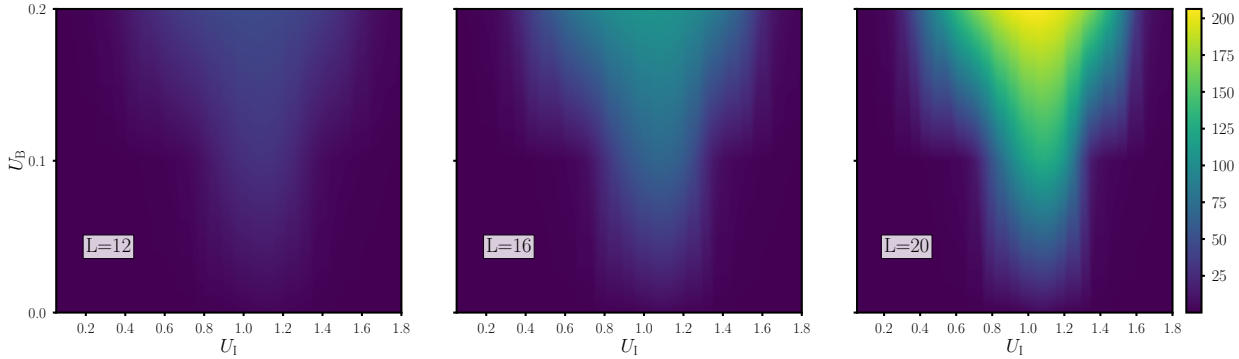


FIG. 3. Evidence for the phase diagram shown in Fig. 1. Shown are heat maps of the susceptibility χ_{ud} at three lattice sizes, illustrating the structure of the phase diagram. Enhanced susceptibilities indicative of an SSB phase are visible for U_B values as small as $U_B = 0.01$ at $U_I = 1.0$ (see [28]).

each lattice site a parity—either even or odd. For generic values of U_I and U_B , the action in Eq. (2) exhibits an $SU(2) \times SU(2) \times U_\chi(1)$ internal symmetry. One of the $SU(2)$ factors mixes u_i and \bar{u}_i according to

$$\begin{pmatrix} u_i \\ \bar{u}_i \end{pmatrix} \rightarrow G_u \begin{pmatrix} u_i \\ \bar{u}_i \end{pmatrix}, \quad \begin{pmatrix} \bar{u}_j \\ u_j \end{pmatrix} \rightarrow G_u^* \begin{pmatrix} \bar{u}_j \\ u_j \end{pmatrix}, \quad (3)$$

where G_u is a 2×2 $SU(2)$ matrix, i denotes an even site, and j denotes an odd site. A second, independent $SU(2)$ matrix G_d acts analogously on the pair (d_i, \bar{d}_i) . The $U_\chi(1)$ symmetry also acts as in Eq. (3), but with G_u replaced by the phase $e^{i\theta}$ and G_d replaced by $e^{-i\theta}$. The SSB phase corresponds to the spontaneous breaking of this $U_\chi(1)$ subgroup.

When $U_B = 0$, the internal symmetry enlarges to $SU(4)$:

$$\begin{pmatrix} u_i \\ \bar{u}_i \\ d_i \\ \bar{d}_i \end{pmatrix} \rightarrow V \begin{pmatrix} u_i \\ \bar{u}_i \\ d_i \\ \bar{d}_i \end{pmatrix}, \quad \begin{pmatrix} \bar{u}_j \\ u_j \\ \bar{d}_j \\ d_j \end{pmatrix} \rightarrow V^* \begin{pmatrix} \bar{u}_j \\ u_j \\ \bar{d}_j \\ d_j \end{pmatrix}, \quad (4)$$

where V is now a 4×4 matrix in $SU(4)$, while the even/odd site structure and the conjugation pattern are identical to those in Eq. (3).

The fact that the two critical lines meet precisely at $U_B = 0$ may therefore be attributed to this symmetry enhancement. Based on this observation, we conjecture that the apparent direct MF-SMG transition is in fact a multicritical point with enlarged $SU(4)$ symmetry.

One of the observables we compute using our Monte Carlo method to study the phase structure is the susceptibility involving the u and d fields,

$$\chi_{ud} = \frac{1}{2V} \sum_{i,j} \langle \bar{u}_i u_i \bar{d}_j d_j \rangle, \quad (5)$$

where $\langle \cdot \rangle$ denotes the path-integral expectation value using the action in Eq. (2). By replacing the d fields with u

fields in Eq. (5), or vice versa, we obtain two additional susceptibilities, χ_{uu} and χ_{dd} . It is easy to verify that $\chi_{uu} = \chi_{dd}$. We also find that χ_{ud} and χ_{uu} are approximately equal on large lattices except for small U_I . Further details regarding the behavior of these susceptibilities are provided in Ref. [28].

Most of our detailed calculations related to the two transitions were performed at $U_B = 0.1$ for various values of U_I near the Gross–Neveu critical point U_I^{GN} and the 3D–XY critical point U_I^{XY} , as indicated in Fig. 1. We discuss our results for the two transitions in detail below. Near both transitions we fit the susceptibility data to the critical scaling form

$$\chi L^{2-\eta} = f((U_I - U_I^c) L^{1/\nu}), \quad (6)$$

where χ denotes either χ_{ud} or χ_{uu} , with each having its own universal scaling function $f(x)$, where $x = (U_I - U_I^c) L^{1/\nu}$.

At the Gross–Neveu transition we set $U_I^c = U_I^{\text{GN}}$ and determine this value together with the corresponding exponents η and ν by performing a combined fit of both χ_{ud} and χ_{uu} data to the scaling form Eq. (6), using a fourth-order polynomial expansion

$$f(x) = f^{(0)} + f^{(1)}x + f^{(2)}x^2 + f^{(3)}x^3, \quad (7)$$

for each susceptibility. Our results for χ_{ud} and the corresponding fit are shown in the left panel of Fig. 2. Statistical errors in the Monte Carlo data have been computed using the jackknife method, and cross-checked using bootstrap as well as autocorrelation corrected errors for consistency. We obtain $U_I^{\text{GN}} = 0.610(1)$, $\nu = 1.06(2)$, and $\eta = 1.00(3)$. The polynomial coefficients entering the universal function in Eq. (7) for χ_{ud} and χ_{uu} are listed in Table I.

The critical exponents we obtain agree within errors with the four-loop ϵ -expansion results [30], with the caveat that the symmetries of our lattice staggered-fermion formulation are not easily captured in most continuum approaches. It is also worth noting that these values lie

	$f^{(0)}$	$f^{(1)}$	$f^{(2)}$	$f^{(3)}$	$f^{(4)}$
χ_{ud}	0.18(2)	0.11(2)	0.06(1)	0.04(1)	0.014(4)
χ_{uu}	0.19(1)	0.11(1)	0.06(1)	0.04(1)	0.015(4)

TABLE I. The first five polynomial coefficients of the universal critical function in Eq. (7) for both χ_{ud} and χ_{uu} . The critical coupling and exponents were included as fit parameters and found to be $U_I^{\text{GN}} = 0.610(1)$, $\nu = 1.06(2)$, and $\eta = 1.00(3)$. The data and corresponding fit are shown in the left panel of Fig. 2.

	$f^{(0)}$	$f^{(1)}$
χ_{ud}	0.1280(2)	-0.0258(1)
χ_{uu}	0.1287(2)	-0.0257(1)

TABLE II. The first two coefficients of the polynomial expansion of the universal critical function in Eq. (8) for both χ_{ud} and χ_{uu} . The exponents $\nu = 0.6715$ and $\eta = 0.0380$ were fixed to their known 3D values, but the critical coupling $U_I^{XY} = 1.2972(1)$ was obtained in the fit. The data and corresponding fit are shown in the right panel of Fig. 2.

close to the large- N_f mean-field predictions $\nu = 1$ and $\eta = 1$ [31]. This Gross–Neveu transition is additionally relevant in the context of twisted bilayer graphene; recent Monte Carlo studies on much smaller lattices report similar exponent values [32]. Other recent theoretical studies also find consistent numbers with small variations. Table I of [33] lists the latest results from several studies.

The presence of the SMG phase at large values of U_I implies a second phase transition, at which the spontaneous breaking of the $U(1)_\chi$ symmetry in the SSB phase is lost while the fermions remain massive and therefore decouple from the critical dynamics. This transition is thus expected to belong to the 3D–XY universality class. Denoting the corresponding critical coupling by $U_I^c = U_I^{XY}$, we determine its value by performing a combined fit of the χ_{ud} and χ_{uu} data to Eq. (6). In this case, a linear approximation to the universal scaling function,

$$f(x) = f^{(0)} + f^{(1)}x, \quad (8)$$

is sufficient. In the fit, we fix the critical exponents to their known 3D–XY values, $\nu = 0.6715$ and $\eta = 0.0380$ [34]. Our results for χ_{ud} , together with the corresponding fit, are shown in the right panel of Fig. 2, and the fitted parameter values are listed in Table II.

To establish that the phase diagram of Eq. (2) is indeed given by Fig. 1, we computed the susceptibilities for various values of U_B and U_I at $L = 12$, $L = 16$, and $L = 20$. The resulting heat maps are shown in Fig. 3. Darker colors correspond to smaller susceptibility values, while lighter colors indicate larger values, with the color scale displayed alongside each plot. These results are consistent with the phase structure summarized in Fig. 1.

To establish that the phase diagram of Eq. (2) is indeed given by Fig. 1, we computed the susceptibilities for

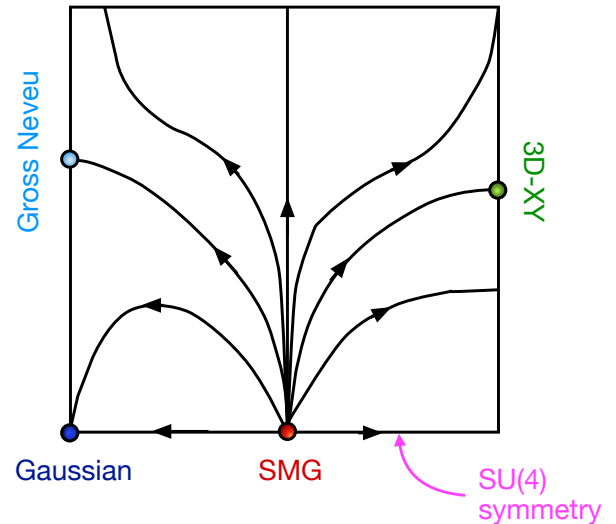


FIG. 4. Conjectured RG flows in three dimensions for fermionic Gross–Neveu–Yukawa models near the SMG fixed point. Our results indicate four fixed points: the Gaussian fixed point (massless fermions, massive bosons); a Gross–Neveu fixed point (interacting massless fermions and bosons, one relevant direction); an XY fixed point (interacting massless bosons, one relevant direction); and the new SMG fixed point, which has two relevant directions but reduces to one when an additional symmetry is imposed.

various values of U_B and U_I at $L = 12$, $L = 16$, and $L = 20$. The resulting heat maps are shown in Fig. 3. Darker colors correspond to smaller susceptibility values, while lighter colors indicate larger values, with the color scale displayed alongside each plot. These results are consistent with the phase structure summarized in Fig. 1.

Based on the results presented here, we find strong support for the interpretation that the 3D Gross–Neveu and 3D–XY critical lines studied in this work merge at a multicritical point, identified as the SMG critical point discovered in earlier studies [6, 7]. This scenario implies the existence of at least four distinct fixed points in the renormalization-group (RG) flow of the associated Gross–Neveu–Yukawa theories with four flavors of four-component massless Dirac fermions, one of which is the SMG fixed point. Our conjectured RG flows are illustrated in Fig. 4, and closely resemble those proposed long ago in [26]. The enhanced $SU(4)$ symmetry at the SMG fixed point plays a crucial role, as it allows the multicritical point to be accessed by tuning a single coupling rather than two, thereby facilitating its identification in earlier lattice studies in three space-time dimensions [6, 7].

Recent perturbative analyses of RG flows near the SMG fixed point have focused on $SU(4)$ -invariant theories [18]. It should, however, be straightforward to extend these studies by including symmetry-breaking terms that reduce the symmetry to $SU(2) \times SU(2) \times U_\chi(1)$ and allow for spontaneous breaking of the $U_\chi(1)$ symmetry. Such an extension would enable a direct test of the RG-flow

structure proposed in Fig. 4.

The model defined by the action Eq. (2) can also be constructed in four space-time dimensions, where the intermediate SSB phase persists even at $U_B = 0$ [9]. This suggests that the SU(4)-enhanced multicritical point identified in three dimensions is a dynamical feature of the renormalization-group flows specific to three space-time dimensions. Although there are preliminary indications that an SMG fixed point may also exist in four dimensions when the model is extended to include Yukawa interactions, provided that two parameters are fine tuned [35], it is not yet established whether its appearance is governed by a similar multicritical point with enhanced symmetry. Clarifying this issue and testing the persistence of any enhanced multicritical structure beyond three dimensions remains an important direction for future work.

ACKNOWLEDGMENTS

We are grateful to Subhro Bhattacharjee, Simon Catterall, Asit De and Cenke Xu for insightful discussions. SC is supported in part by the U.S. Department of Energy,

Office of Science, Nuclear Physics program under Award No. DE-FG02-05ER41368. This research was supported in part by the National Science Foundation under Grant No. NSF PHY-1748958. DB would like to acknowledge continued support from the Alexander von Humboldt Foundation (Germany) in the context of the research fellowship for experienced researchers. MKM is grateful for the hospitality of Perimeter Institute where part of this work was carried out. Research at Perimeter Institute is supported in part by the Government of Canada through the Department of Innovation, Science and Economic Development and by the Province of Ontario through the Ministry of Colleges and Universities. This research was also supported in part by the Simons Foundation through the Simons Foundation Emmy Noether Fellows Program at Perimeter Institute. SM would like to thank the Institute for Theoretical Physics at ETHZ for hospitality during his visit, where part of this work was carried out. DB, SM and MKM also acknowledge the use of computing clusters at SINP, Kolkata, and access to the Piz Daint and Eiger supercomputers at the Swiss National Supercomputing Centre, Switzerland, under ETHZ's allocation with project IDs **c21** and **eth8**.

[1] D. J. Gross and A. Neveu, Dynamical Symmetry Breaking in Asymptotically Free Field Theories, *Phys. Rev. D* **10**, 3235 (1974).

[2] A. Hasenfratz, W.-q. Liu, and T. Neuhaus, Phase Structure and Critical Points in a Scalar Fermion Model, *Phys. Lett. B* **236**, 339 (1990).

[3] I.-H. Lee, J. Shigemitsu, and R. E. Shrock, Study of Different Lattice Formulations of a Yukawa Model With a Real Scalar Field, *Nucl. Phys. B* **334**, 265 (1990).

[4] W. Bock, A. K. De, K. Jansen, J. Jersak, T. Neuhaus, and J. Smit, Phase Diagram of a Lattice SU(2) X SU(2) Scalar Fermion Model With Naive and Wilson Fermions, *Nucl. Phys. B* **344**, 207 (1990).

[5] K. Slagle, Y.-Z. You, and C. Xu, Exotic quantum phase transitions of strongly interacting topological insulators, *Phys. Rev. B* **91**, 115121 (2015), arXiv:1409.7401 [cond-mat.str-el].

[6] V. Ayyar and S. Chandrasekharan, Massive fermions without fermion bilinear condensates, *Phys. Rev. D* **91**, 065035 (2015), arXiv:1410.6474 [hep-lat].

[7] V. Ayyar and S. Chandrasekharan, Origin of fermion masses without spontaneous symmetry breaking, *Phys. Rev. D* **93**, 081701 (2016), arXiv:1511.09071 [hep-lat].

[8] S. Catterall, Fermion mass without symmetry breaking, *JHEP* **01**, 121, arXiv:1510.04153 [hep-lat].

[9] V. Ayyar and S. Chandrasekharan, Fermion masses through four-fermion condensates, *JHEP* **10**, 058, arXiv:1606.06312 [hep-lat].

[10] Y.-Y. He, H.-Q. Wu, Y.-Z. You, C. Xu, Z. Y. Meng, and Z.-Y. Lu, Quantum critical point of Dirac fermion mass generation without spontaneous symmetry breaking, *Phys. Rev. B* **94**, 241111 (2016), arXiv:1603.08376 [cond-mat.str-el].

[11] N. Butt, S. Catterall, and G. C. Toga, Symmetric Mass Generation in Lattice Gauge Theory, *Symmetry* **13**, 2276 (2021), arXiv:2111.01001 [hep-lat].

[12] N. Butt, S. Catterall, and A. Hasenfratz, Symmetric Mass Generation with Four SU(2) Doublet Fermions, *Phys. Rev. Lett.* **134**, 031602 (2025), arXiv:2409.02062 [hep-lat].

[13] A. Hasenfratz and O. Witzel (Lattice Strong Dynamics), Symmetric Mass Generation, in *2025 European Physical Society Conference on High Energy Physics* (2025) arXiv:2511.22678 [hep-lat].

[14] S. S. Razamat and D. Tong, Gapped chiral fermions, *Phys. Rev. X* **11**, 011063 (2021).

[15] D. Tong, Comments on symmetric mass generation in 2d and 4d, *JHEP* **07**, 001, arXiv:2104.03997 [hep-th].

[16] J. Wang and Y.-Z. You, Symmetric Mass Generation, *Symmetry* **14**, 1475 (2022), arXiv:2204.14271 [cond-mat.str-el].

[17] Y.-Z. You, Y.-C. He, C. Xu, and A. Vishwanath, Symmetric fermion mass generation as deconfined quantum criticality, *Phys. Rev. X* **8**, 011026 (2018).

[18] S. Martin and T. Grover, A Perturbative Approach to Symmetric Mass Generation, preprint (2025), arXiv:2507.23032 [cond-mat.str-el].

[19] E. Eichten and J. Preskill, Chiral Gauge Theories on the Lattice, *Nucl. Phys. B* **268**, 179 (1986).

[20] J. Wang and X.-G. Wen, A Solution to the 1+1D Gauged Chiral Fermion Problem, *Phys. Rev. D* **99**, 111501 (2018), arXiv:1807.05998 [hep-lat].

[21] Y. Xu and C. Xu, Green's function Zero and Symmetric Mass Generation, preprint (2021), arXiv:2103.15865 [cond-mat.str-el].

[22] M. Zeng, Z. Zhu, J. Wang, and Y.-Z. You, Symmetric Mass Generation in the 1+1 Dimensional Chiral Fermion 3-4-5-0 Model, *Phys. Rev. Lett.* **128**, 185301 (2022),

arXiv:2202.12355 [cond-mat.str-el].

[23] M. Golterman and Y. Shamir, Propagator Zeros and Lattice Chiral Gauge Theories, *Phys. Rev. Lett.* **132**, 081903 (2024), arXiv:2311.12790 [hep-lat].

[24] M. Golterman and Y. Shamir, Constraints on the symmetric mass generation paradigm for lattice chiral gauge theories, preprint (2025), arXiv:2505.20436 [hep-lat].

[25] R. Moulard, D. Tong, and B. Zan, Phases of 2d Gauge Theories and Symmetric Mass Generation, preprint (2025), arXiv:2509.12305 [hep-th].

[26] A. Hasenfratz and T. Neuhaus, Nonperturbative Study of the Strongly Coupled Scalar Fermion Model, *Phys. Lett. B* **220**, 435 (1989).

[27] H. S. Sharatchandra, H. J. Thun, and P. Weisz, Susskind Fermions on a Euclidean Lattice, *Nucl. Phys. B* **192**, 205 (1981).

[28] S. Maiti, D. Banerjee, S. Chandrasekharan, and M. K. Marinkovic, Phase diagram of a lattice fermion model with symmetric mass generation, companion paper.

[29] S. Chandrasekharan, The Fermion bag approach to lattice field theories, *Phys. Rev. D* **82**, 025007 (2010), arXiv:0910.5736 [hep-lat].

[30] N. Zerf, L. N. Mihaila, P. Marquard, I. F. Herbut, and M. M. Scherer, Four-loop critical exponents for the gross-neveu-yukawa models, *Phys. Rev. D* **96**, 096010 (2017).

[31] S. Hands, A. Kocic, and J. B. Kogut, Four Fermi theories in fewer than four-dimensions, *Annals Phys.* **224**, 29 (1993), arXiv:hep-lat/9208022.

[32] C. Huang, N. Parthenios, M. Ulybyshev, X. Zhang, F. F. Assaad, L. Classen, and Z. Y. Meng, Angle-tuned gross-neveu quantum criticality in twisted bilayer graphene, *Nature Communications* **16**, 7176 (2025).

[33] B. Hawashin, M. M. Scherer, and L. Janssen, Gross-neveu-XY quantum criticality in moiré dirac materials, *Phys. Rev. B* **111**, 205129 (2025).

[34] M. Campostrini, M. Hasenbusch, A. Pelissetto, P. Rossi, and E. Vicari, Critical behavior of the three-dimensional XY universality class, *Phys. Rev. B* **63**, 214503 (2001).

[35] N. Butt, S. Catterall, and D. Schaich, $SO(4)$ invariant Higgs-Yukawa model with reduced staggered fermions, *Phys. Rev. D* **98**, 114514 (2018), arXiv:1810.06117 [hep-lat].